PHYSICAL REVIEW C VOLUME 32, NUMBER 4 OCTOBER 1985

Final state interactions and relativistic effects in the $(\vec{e},e'p)$ reaction

A. Picklesimer*
Department of Physics and Astronomy, University of Maryland, College Park, Maryland 20742 and Los Alamos National Laboratory, Los Alamos, New Mexico 87545

J. W. Van Orden and S. J. Wallace
Department of Physics and Astronomy, University of Maryland, College Park, Maryland 20742
(Received 24 May 1985)

The five response functions which characterize the $(\vec{e},e'p)$ reaction are calculated in the distorted wave impulse approximation using a Dirac equation formulation of the nuclear bound and scattering wave functions and the usual free Dirac current operator. By evaluating the current matrix elements in momentum space, it is possible to recover the traditional Schrödinger dynamics and thus to study off-shell effects from the proton-nucleus final state interaction in both the relativistic and the nonrelativistic approaches. The longitudinal response function with relativistic effects included is reduced by about 20 percent relative to the nonrelativistic results. This is shown to be due to the Dirac final state interaction. Relativistic nuclear bound-state effects are found to be small in this reaction. The other four response functions show relativistic effects on the order of 5 to 10 percent. Off-shell effects are shown to be especially important in the interference response functions. A rough measure of the violation of current conservation in such calculations is presented and its implications for the calculations are discussed.

I. INTRODUCTION

Analyses of (e,e'p) reactions have been made in attempts to learn about spectroscopic factors, spectral functions, and momentum-space wave functions.[1,2] Generally, the analyses[3] are carried out in a nonrelativistic framework using a reduction of the relativistic current operator appropriate to nonrelativistic Schrödinger wave functions for the bound state and the ejected proton. The reduction of the relativistic current operator is obtained by truncation of an expansion in p/m. Moreover, the models generally used involve the impulse approximation, i.e., the use of free one-body current operators, and distorted waves for the ejected proton which are based on a simple optical potential. These approximations reduce the calculation to manageable form, however, it is clear that a treatment involving considerably more complexity is ultimately needed.

In this paper, we consider $(\vec{e},e'p)$ reactions using a relativistic format. Both the bound state and the final state distorted wave are based on the Dirac equation, which implicitly includes pair effects. The electromagnetic current operator for one-photon exchange is used in its elementary form without a p/m expansion. Therefore, the analysis has essentially the same ingredients as the traditional Schrödinger approach with the exception that everything is done in the framework of relativistic dynamics. Recent developments have given substantial credence to a relativistic nuclear dynamics in which the nucleon-nucleus interaction is characterized by large scalar and vector potentials in the Dirac equation.[4–7] The Dirac approach provides improved descriptions of spin observables in proton-nucleus elastic scattering. Moreover, simple Hartree-approximation calculations provide nuclear densities which are in good accord with electron scattering data.[8,9] The Dirac scalar and vector potentials are of opposite sign and they provide a natural explanation of the spin-orbit splitting in nuclear shells.[10] Since the scalar and vector potentials are large, the usual reduction of the electromagnetic current matrix element to an effective nonrelativistic form using free Dirac spinors may omit significant effects.[11] We test this possibility by performing a straightforward relativistic analysis of the $(\vec{e},e'p)$ reaction.

Currently, one of the important issues in electromagnetic physics is the explanation of the observed quenching of the longitudinal response function relative to the transverse response function in (e,e') inclusive scattering.[12,13] Various authors have identified the quenching as a natural consequence of the relativistic approach, at least in part.[14–16] However, these analyses were based on crude modes such as infinite nuclear matter or they employed phenomenological parameters.[16] One of our objectives is to examine the extent to which the quenching is present in microscopically calculated $(\vec{e},e'p)$ reactions and to explore the possibility that the three new response functions[17–19] of this reaction may shed new light on possible relativistic effects. The five response functions of the $(\vec{e},e'p)$ reaction are calculated using relativistic Hartree wave functions[8,9] for the bound state and microscopic Dirac optical model wave functions for the knockout proton.[6,7] The final state optical potential is based on free nucleon-nucleon amplitudes and a nuclear density which is obtained from elastic electron scattering data. There are no adjustable parameters. The analysis is done completely in momentum space. This procedure permits a clean separation of relativistic versus nonrelativistic distortion and bound-state effects and also a clean separation

of on-shell versus off-shell final state scattering effects. Substantial quenching of the longitudinal response function is found in our $(\vec{e},e'p)$ analysis, however, very little of it arises from the use of relativistic bound state wave functions. Rather, the relativistic final state interaction seems to provide the dominant quenching mechanism.

However, some caution should be exercised in comparing our calculated results with experimental data [this is true of all distorted wave impulse approximation (DWIA) calculations]. A consistent treatment of the hadronic current operator and the hadronic wave functions is needed in order to conserve the electromagnetic current, whereas the present analysis omits correlation contributions and meson exchange currents consistent with the interaction potential. Further investigations are planned to extend the analysis at least to the 2p-2h level, however, the scope of the present work is limited to an exploration of relativistic and other dynamical effects in DWIA. In addition, Coulomb distortion of the ejected proton is omitted in the present work in order to simplify the dynamical investigations which are the focal point of this paper. This omission is not expected to lead to significant alteration of our results. It will be removed in subsequent investigations.

In Sec. II of this paper, the basic formalism of the $(\vec{e},e'p)$ reaction is reviewed. A brief outline of the derivation of the cross section for this reaction is presented and the response functions[17,18] are defined in terms of matrix elements of the nuclear electromagnetic current operator. The analysis in this section incorporates the helicity dependent response function first pointed out by Donnelly.[19] This analysis serves mainly to define the notation and conventions which are used throughout this paper.

Section III contains a discussion of theoretical aspects of the $(\vec{e},e'p)$ reaction and our calculational approach. The independent particle, DWIA approximation to the nuclear current matrix elements is discussed and the implications of this approximation for electromagnetic current conservation are examined. The Dirac shell-model wave functions used in this calculation are discussed and the choice of a one-body Dirac electromagnetic current operator is described. The construction of the relativistic distorted proton waves is then described. We discuss various approximations and limiting cases which elucidate the important physical mechanisms in the $(\vec{e},e'p)$ reaction and which can be obtained from our momentum-space calculations.

Section IV contains a presentation of the numerical results. Calculations of the five response functions for the ejection of 135 MeV protons from the $1p_{1/2}$ and $1p_{3/2}$ shells of ^{16}O are presented. Comparisons of relativistic, nonrelativistic, on-shell, and plane wave calculations are made for each response function. Relativistic effects and possible off-shell sensitivities are discussed. A measure of the violation of current conservation is presented.

In Sec. V, conclusions reached as a result of our investigations are presented.

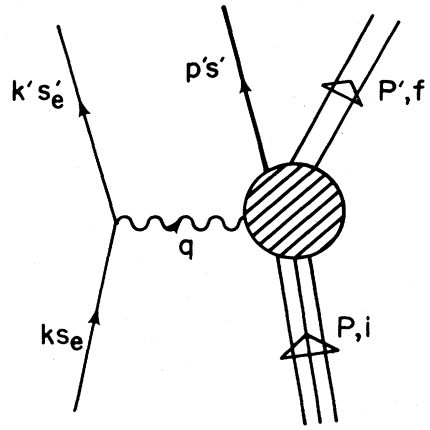

FIG. 1. Schematic diagram of the (e,e'p) reaction.

II. ELECTRON SCATTERING FORMALISM

The one-photon exchange mechanism provides a good approximation to elastic and inelastic electron scattering from light and medium sized nuclei. With this approximation a general form of the $(\vec{e},e'p)$ cross section can be determined by means of fairly simple and straightforward arguments. In order to present some of the notation which will be used throughout this paper, it is useful to present a brief outline of the derivation of $(\vec{e},e'p)$ cross section.[17–19]

In the one-photon exchange approximation, the $(\vec{e},e'p)$ reaction is schematically represented by Fig. 1. In this figure, k and k' represent the initial and final electron four-momenta and s_e and s'_e represent the initial and final electron spin. The four-momentum transferred to the nuclear system by the absorption of the virtual photon is represented by q. P and P' represent the four-momenta of the target and residual nucleus, while the quantum numbers of the intrinsic states, ψ_{iP} and $\psi_{fP'}$, are labeled by i and f, respectively. The four-momentum and spin of the ejected proton are labeled by p' and s'. In terms of these quantities, the $(\vec{e},e'p)$ differential cross section (final spins unobserved) in the target rest frame can be written as

$$d\sigma=\frac{m_e}{|\mathbf{k}|}\frac{m_e d^3k'}{(2\pi)^3\epsilon_{k'}}\frac{m d^3p'}{(2\pi)^3E_{p'}}\sum_{s'_e}\sum_{f}\sum_{s'}\sum_{i}\int\frac{d^3P'}{(2\pi)^3}\Phi_f(\mathbf{P}')(2\pi)^4\delta^4(k-k'+P-P'-p')$$
$$\times\left|\bar{u}(k's'_e)\gamma_\mu u(ks_e)\frac{e^2}{q^2}\langle p's'(-),\psi_{fP'}|\hat{J}^\mu(q)|\psi_{iP}\rangle\right|^2, \tag{2.1}$$

where m_e and m are the electron and nucleon masses, $\epsilon_{k'}=(\mathbf{k}'^2+m_e^2)^{1/2}$, and $E_{p'}=(\mathbf{p}'^2+m^2)^{1/2}$. The electron spinors and gamma matrices follow the standard conventions.[20] $\Phi_f(\mathbf{P}')$ is a density of states factor appropriate for the intrinsic

spin of the residual nucleus. In our case, since the recoil momentum is nonrelativistic, $\Phi_f(\mathbf{P}')=1$. The electron charge is e and $\hat{J}^\mu(q)$ is the electromagnetic current operator for the nuclear system appropriate to the particular choice of dynamics and basis states for the nuclear system. The incoming (spherical) wave boundary condition is appropriate for the continuum part of the final state and this is indicated by the $(-)$ in (2.1). The notation $\overline{\sum}$ indicates an average over allowed states.

It is conventional to separate the electron and nuclear components of the cross section by defining an electron tensor

$$\eta_{\mu\nu}=m_e^2\sum_{s_e'}\bar{u}(ks_e)\gamma_\mu u(k's_e')\bar{u}(k's_e')\gamma_\nu u(ks_e) \tag{2.2}$$

and a nuclear tensor

$$W^{\mu\nu}=\sum_f\sum_{s'}\overline{\sum_i}\int\frac{d^3P'}{(2\pi)^3}\Phi_f(\mathbf{P}')(2\pi)^3\delta^4(k-k'+P-P'-p')$$
$$\times\langle\psi_{iP}\,|\,\hat{J}^{\mu\dagger}(q)\,|\,p's'(-),\psi_{fP'}\rangle\langle p's'(-),\psi_{fP'}\,|\,\hat{J}^\nu(q)\,|\,\psi_{iP'}\rangle\ . \tag{2.3}$$

These two second-rank tensors are determined by bilinear combinations of the electron and nuclear electromagnetic currents, respectively. In terms of these tensors, the contribution of the absolute square of the matrix elements in (2.1) is contained in

$$\frac{e^4}{m_e^2q^4}\eta_{\mu\nu}W^{\mu\nu}\ . \tag{2.4}$$

The electron tensor can be explicitly calculated using the spin projection operator for the incident electron and simple trace theorems. In the extreme relativistic limit (ERL), which is appropriate for electrons with energies in the region of interest for this work, this gives[21]

$$\eta_{\mu\nu}=\tfrac{1}{8}\,\mathrm{tr}[\gamma_\mu k'\gamma_\nu(1+h\gamma_5)k]\ ,$$
$$=(k'_\mu k_\nu+k'_\nu k_\mu-k'\cdot kg_{\mu\nu}+hi\epsilon_{\mu\nu\lambda\kappa}k'^{\lambda}k^{\kappa})/2\ , \tag{2.5}$$

where h is $+1$ for positive electron helicity and -1 for negative electron helicity. The sum of the first three terms of (2.5) is symmetric with respect to the interchange of μ and ν and is independent of the electron helicity. This sum is identical to the electron tensor obtained for the case of unpolarized incident electrons. The last term is antisymmetric under interchange of μ and ν, and depends linearly on the electron helicity. The electron tensor can therefore be written as the sum of a symmetric and an antisymmetric tensor, where only the antisymmetric tensor depends on the initial electron helicity.

$$\eta_{\mu\nu}=\eta^S_{\mu\nu}+\eta^A_{\mu\nu}\ . \tag{2.6}$$

A general form for the nuclear tensor can be constructed using simple invariance arguments. In the case where the spins of the final nucleon and nucleus are not observed, this tensor must be constructed from the three linearly independent four vectors q, p', and P, the scalars that can be constructed from them, q^2, $q\cdot P$, $q\cdot p'$, and $p'\cdot P$, and the second-rank tensor $g_{\mu\nu}$. The fact that only three independent four-vectors are available precludes a scalar constructed from, and linear in, the completely antisymmetric tensor $\epsilon_{\mu\nu\rho\sigma}$, while second-rank tensors constructed from the available four-vectors and linear in $\epsilon_{\mu\nu\rho\sigma}$ are inconsistent with a parity conserving electromagnetic current. Scalars and tensors bilinear in ϵ are not linearly independent of the indicated set. Electromagnetic current conservation requires, in addition, that

$$q_\mu W^{\mu\nu}=q_\nu W^{\mu\nu}=0\ . \tag{2.7}$$

This constraint is most easily satisfied by constructing $W^{\mu\nu}$ from a complete set of four-vectors and second-rank tensors which individually satisfy the same constraint. These "gauge invariant forms" are

$$G^{\mu\nu}=g^{\mu\nu}-\frac{q^\mu q^\nu}{q^2}\ ,$$
$$V_i^\mu=\frac{1}{M_T}\left[P^\mu-\frac{P\cdot q}{q^2}q^\mu\right]\ , \tag{2.8}$$
$$V_f^\mu=\left[P'^\mu-\frac{P'\cdot q}{q^2}q^\mu\right]\ .$$

The nuclear tensor can then be written as

$$W^{\mu\nu}=W_1G^{\mu\nu}+W_2V_i^\mu V_i^\nu+W_3V_f^\mu V_f^\nu+W_4(V_i^\mu V_f^\nu+V_f^\mu V_i^\nu)$$
$$+W_5(V_i^\mu V_f^\nu-V_f^\mu V_i^\nu)\ , \tag{2.9}$$

where the W_i are functions of the available Lorentz scalars. As in the case of the electron tensor, this can be written as the sum of a symmetric part consisting of the first four terms and an antisymmetric part consisting of the last term,

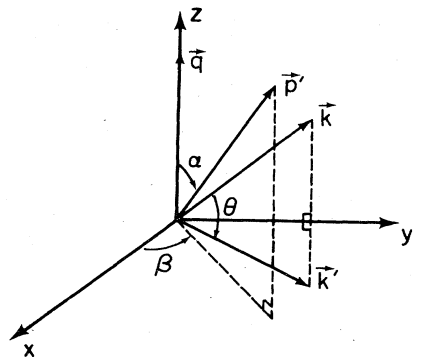

FIG. 2. Coordinate axes used to define the angles α and β.

$$W^{\mu\nu}=W^{\mu\nu S}+W^{\mu\nu A}\ . \tag{2.10}$$

Since the contraction of a symmetric and an antisymmetric tensor yields zero, the contraction of the electron and nucleon tensors can be written as

$$\eta_{\mu\nu}W^{\mu\nu}=\eta^{S}_{\mu\nu}W^{\mu\nu S}+\eta^{A}_{\mu\nu}W^{\mu\nu A}\ . \tag{2.11}$$

The cross section for unpolarized electrons is thus determined by only the symmetric part of the nuclear tensor. The antisymmetric part of the nuclear tensor can be "seen" only with polarized electrons.

Choosing the coordinate system shown in Fig. 2 and using the kinematics of the scattered electron, the differential cross section for the creation of a proton hole state by an incident electron with helicity h can be written as,

$$\left[\frac{d^3\sigma}{d\epsilon_{k'}d\Omega_{k'}d\Omega_{p'}}\right]_h=\frac{m\,|\mathbf{p}'|}{(2\pi)^3}\left[\frac{d\sigma}{d\Omega_{k'}}\right]_{\text{Mott}}\left[\frac{q^4}{\mathbf{q}^4}R_L+\left[\tan^2\frac{\theta}{2}-\frac{q^2}{2\mathbf{q}^2}\right]R_T-\frac{q^2}{2\mathbf{q}^2}\cos2\beta R_{TT}+\frac{q^2}{\mathbf{q}^2}\right.$$
$$\left.\times\left[\tan^2\tfrac{8}{2}-\frac{q^2}{\mathbf{q}^2}\right]^{1/2}\sin\beta R_{LT}+h\frac{q^2}{\mathbf{q}^2}\tan\frac{\theta}{2}\cos\beta R_{LT'}\right]\ , \tag{2.12}$$

where $q^2=\omega^2-\mathbf{q}^2$ and $\omega=q^0$ is the energy transfer. The Mott cross section, which is the cross section for electron scattering from an infinitely massive point "nucleon" is defined in the ERL by

$$\left[\frac{d\sigma}{d\Omega_{k'}}\right]_{\text{Mott}}=\frac{\alpha^2\cos^2\theta/2}{4\,|\mathbf{k}|^2\sin^4\theta/2}\ , \tag{2.13}$$

where here α is the fine structure constant. The quantities R_L, R_T, R_{TT}, R_{LT}, and $R_{LT'}$ are the longitudinal, transverse, transverse-transverse, longitudinal-transverse, and polarized longitudinal-transverse response functions, respectively. These five response functions are defined in terms of the components of the nuclear tensor integrated over a line width in the missing mass spectrum as follows:

$$\begin{aligned}
R_L&=\int_{\text{line}}dE_{p'}W^{00}\ ,\\
R_T&=\int_{\text{line}}dE_{p'}(W^{11}+W^{22})=\int_{\text{line}}dE_{p'}(W^{++}+W^{--})\ ,\\
\cos2\beta R_{TT}&=\int_{\text{line}}dE_{p'}(W^{22}-W^{11})\\
&=\int_{\text{line}}dE_{p'}2\,\text{Re}(W^{+-})\ ,\\
\sin\beta R_{LT}&=\int_{\text{line}}dE_{p'}(W^{02}+W^{20})\\
&=-\int_{\text{line}}dE_{p'}2^{1/2}\,\text{Im}(W^{0+}+W^{0-})\ ,\\
\cos\beta R_{LT'}&=\int_{\text{line}}dE_{p'}i(W^{10}-W^{01})\\
&=\int_{\text{line}}dE_{p'}2^{1/2}\,\text{Im}(W^{0-}-W^{0+})\ ,
\end{aligned} \tag{2.14}$$

where the response functions have been expressed in terms of a spherical basis,[17] defined by the basis vectors $e^{\pm}=\mp2^{-1/2}(e^1\pm ie^2)$, as well as the Cartesian basis shown in Fig. 2. The response functions are defined so as to be independent of the azimuthal angle β.

Current conservation, which in momentum space can be expressed as $\omega J^0=q\cdot\mathbf{J}$, can be used to eliminate the component of the three-vector current parallel to the momentum transfer in favor of the charge density. This has been used in deriving (2.12). Thus, longitudinally polarized virtual photons couple to the nuclear transition charge density J^0, while virtual photons with helicity ±1 couple to the two components $J^{\pm}$ of the three-vector transition current density transverse to the direction of the photon. Since all three independent components of the four-vector current can exist for a given transition, response functions which involve the interference of the various current components are present. Remembering the definition of $W^{\mu\nu}$, the response function R_L is determined entirely by the transition charge density. The response function R_T is given by the sum of the squares of the two transverse components of the transition current density. This corresponds to summing over the photon helicities ±1. The response function R_{TT} is the result of interference between the two different transverse components of the nuclear electromagnetic current. The response functions R_{LT} and $R_{LT'}$ are the result of interference between the transition charge density and the two transverse components of the current. The azimuthal angular dependence in (2.12) arises as a result of the helicity of the absorbed virtual photon. In inclusive scattering, where terms involving β do not appear due to the azimuthal angle integration, it is only possible to differentiate between the transverse and longitudinal polarizations of the virtual photon, not between the ±1 helicity states of the photon. Since the last three response functions are the result of interference between various components of the nuclear electromagnetic current, they may be expected to be especially sensitive to relative phase differences introduced by the interaction of the ejected nucleon with the rest of the nuclear system. These response functions may, therefore, provide a relatively sensitive test of the nucleon-nucleus final state interaction. Indeed, it is easy to show within the context of a one particle DWIA model that the response function $R_{LT'}$ is identically zero unless there is a final state interaction.

In the coordinate system shown in Fig. 2, the ejected proton is in the scattering plane of the electrons when $\beta=\pm\pi/2$. From the expression for the cross section (2.12), it is clear that, in the scattering plane, all terms contribute, except the term proportional to $R_{LT'}$. This contribution can be detected only with a polarized electron beam and with a spectrometer capable of detecting protons not in the electron scattering plane. Because this term is proportional to the electron helicity, it can be separated from the rest of the cross section by taking the difference between cross sections for each of the two possible incident electron helicities. The term proportional to

R_{LT}, on the other hand, changes sign upon changing the azimuthal angle from $\beta=\pi/2$ to $\beta=-\pi/2$. All of the other terms in (2.11) which contribute in the scattering plane retain the same sign under this change of angle. R_{LT} can therefore be separated by measuring the two cross sections which have the proton in the scattering plane and on either side of the momentum transfer vector $\mathbf{q}$ and then taking the difference between the two cross sections. The term proportional to R_{TT} can be separated only by measuring the cross section at several values of β. The separation of R_L and R_T requires a Rosenbluth separation.

From the discussion presented above, it is clear that the cross section for $(\vec{e},e'p)$ can be determined if the matrix elements of the components of the electromagnetic four-vector current operator are known. In principle, calculation of these matrix elements requires the complete solution of the nuclear many-body problem together with the use of the exact nuclear electromagnetic current operator. These aspects, taken together, represent an exceedingly difficult problem. In practice, it is clearly necessary to introduce severe approximations. In the following section we discuss the approximation of the nuclear current matrix elements using an independent particle DWIA approach.

III. THE NUCLEAR CURRENT MATRIX ELEMENT

The considerations of the previous section resulted in the identification of a set of nuclear response functions which contain the information of central interest in the $(\vec{e},e'p)$ reaction. In order to obtain theoretical predictions of these response functions, it is necessary to compute the matrix elements of the hadronic electromagnetic current operator $\hat{J}^\mu$:

$$J^\mu=\langle p's'(-),\psi_{fP'}\mid\hat{J}^\mu\mid\psi_{iP}\rangle\ , \tag{3.1}$$

where $\mid\psi_{iP}\rangle$ represents the intrinsic initial A-body nuclear ground state vector together with its barycentric momentum P, and $\mid p's'(-),\psi_{fP'}\rangle$ represents the final (stationary state) scattering state vector of the A-body nuclear Hamiltonian with incoming (spherical) wave boundary conditions [denoted by the $(-)$] and target recoil momentum P'. From a time-dependent viewpoint, the final state corresponds to a complicated initial superposition of incoming waves which evolves to an asymptotically simple wave consisting of the relative plane-wave motion of a proton with momentum $\mathbf{p}'$ and spin-projection s' and the final $(A\text{-}1)$-body nuclear bound state f.

For calculational purposes, we follow the usual procedure of approximating $\mid p's'(-),\psi_{fP'}\rangle$ by its single-channel optical model wave function $\mid\psi^{(-)}_{p's'},fP'\rangle$ which is the product of the final nuclear bound state, a "distorted wave" of relative motion and the barycentric motion of the whole system. Relevant aspects of the relativistic optical model approach are discussed in Sec. III A. For the initial bound state, a single-particle shell-model (SM) wave function $\mid\psi^{\rm SM}_i,P\rangle$ is employed. Formally, the exact wave functions can be written in terms of the model wave functions as

$$\langle p's'(-),\psi_{fP'}\mid=\langle\psi^{(-)}_{p's'},fP'\mid\Omega^\dagger_S \tag{3.2}$$

and

$$\mid\psi_i\rangle=\Omega_B\mid\psi^{\rm SM}_i,P\rangle\ , \tag{3.3}$$

where Ω_S and Ω_B are Moller-type wave operators which "evolve" the exact states from the model scattering and bound states.[22] Therefore (3.1) can be rewritten as

$$J^\mu=\langle\psi^{(-)}_{p's'},f\mid\Omega^\dagger_S\hat{J}^\mu\Omega_B\mid\psi^{\rm SM}_i\rangle \tag{3.4}$$

which is still exact. From (3.4) on, we suppress the initial and final nuclear momenta for the sake of notational convenience. Their implicit presence should, however, not be forgotten. The complexity associated with the exact wave functions has been eliminated at the expense of creating an effective current operator

$$\hat{J}^\mu_{\rm eff}=\Omega^\dagger_S\hat{J}^\mu\Omega_B \tag{3.5}$$

which is an extremely complicated object. The usual DWIA approach corresponds to replacing the operators Ω_S and Ω_B by unit operators and the exact nuclear electromagnetic current operator $\hat{J}^\mu$ by a one-body current operator $\hat{J}^{(1)\mu}$. Following this approach, we approximate (3.1) as

$$J^\mu\cong J^\mu_a=\langle\psi^{(-)}_{p's'},f\mid\hat{J}^{(1)\mu}\mid\psi^{\rm SM}_i\rangle\ . \tag{3.6}$$

The shortcomings of omitting the many-body components of the current (3.5) are potentially severe, particularly in regard to electromagnetic current conservation. Estimates of the importance of this problem are presented together with our results in Sec. IV. No existing DWIA calculation of this process conserves current.

In evaluating (3.6), it is necessary to choose a representation. Our calculations are performed entirely in momentum space ($\mathbf{k}$ space), for the following three reasons. First, the isolation and determination of the physical sources of differences between the relativistic and nonrelativistic approaches examined herein, for both the distorted waves and bound states, is most easily accomplished in $\mathbf{k}$ space where the Dirac wave functions can be readily decomposed into positive and negative energy components. Second, the final state scattering of the ejected proton by the residual nucleus can be easily separated into an on-shell part and an off-shell part. The on-shell part is closely constrained by proton-nucleus elastic scattering experiments and therefore $(\vec{e},e'p)$ results in the DWIA should be particularly reliable when final state interaction effects are dominated by the on-shell part. Correspondingly, the importance of the off-shell amplitude can be determined. Third, we intend to extend our studies to other reactions [e.g., (p,γ)] and to the incorporation of meson-exchange currents, the natural setting for which is $\mathbf{k}$ space. In momentum space, neglecting target recoil, (3.6) can be written as

$$J^\mu=\int\frac{d^3p}{(2\pi)^3}\bar{\psi}^{(-)}_{p's'}(\mathbf{p})J^{(1)\mu}(q)\psi^{\rm SM}_i(\mathbf{p}-\mathbf{q})\ . \tag{3.7}$$

In writing (3.7), it has been assumed that the single particle wave functions are four-component Dirac wave functions where $\bar{\psi}$ denotes the usual Dirac conjugate $\psi^\dagger\gamma^0$. The current operator is the usual free Dirac current operator

$$J^{(1)\mu}(q)=\gamma^0\hat{J}^{(1)\mu}(q)=F_1(q^2)\gamma^\mu+\frac{F_2(q^2)}{2m}i\sigma^{\mu\nu}q_\nu\ , \tag{3.8}$$

where F_1 and F_2 are the electromagnetic form factors of the nucleon. The momentum-space Dirac-Hartree wave functions are obtained by Fourier transformation of the coordinate space wave functions of Ref. 8. Following the conventions of Ref. 8, consider a typical bound state solution of the Dirac equation ($\sigma_r=\sigma\cdot\hat{\mathbf{r}}$),

$$\psi^m_{nlj}(\mathbf{r})=\frac{1}{r}\begin{bmatrix}F_{nlj}(r)\\ -i\sigma_r G_{nlj}(r)\end{bmatrix}Y^m_{lj}(\hat{\mathbf{r}})\ , \tag{3.9}$$

where n is the principle quantum number, l is the orbital angular momentum, j is the total angular momentum, m is the z projection of the total angular momentum, and $Y^m_{lj}(\hat{\mathbf{r}})$ is a spin spherical harmonic. These states are normalized as follows

$$\begin{aligned}1&=\int d^3r[\psi^m_{nlj}(\mathbf{r})]^\dagger\psi^m_{nlj}(\mathbf{r})\ ,\\ &=\int_0^\infty dr[F^2_{nlj}(r)+G^2_{nlj}(r)]\ .\end{aligned} \tag{3.10}$$

The momentum-space wave function is

$$\begin{aligned}\psi_i(\mathbf{p})&=\int d^3r e^{-i\mathbf{p}\cdot\mathbf{r}}\psi^m_{nlj}(\mathbf{r})\\ &=\begin{bmatrix}\psi_{i1}(p)\ Y^m_{l_1j}(\hat{\mathbf{p}})\\ \psi_{i2}(p)\ \ Y^m_{l_2j}(\hat{\mathbf{p}})\end{bmatrix}\ ,\end{aligned} \tag{3.11}$$

where

$$\begin{aligned}\psi_{i1}(p)&=(-i)^l4\pi\int_0^\infty dr\, rj_l(pr)F_{nlj}(r)\ ,\\ \psi_{i2}(p)&=i(-1)^{l_2}4\pi\int_0^\infty dr\, rj_{1/2}(pr)G_{nlj}(r)\ .\end{aligned} \tag{3.12}$$

Here $l_1=1$ and $l_2=2j-1$. The normalization of the momentum space wave function is thus

$$\begin{aligned}1&=\int\frac{d^3p}{(2\pi)^3}\psi^\dagger_i(\mathbf{p})\psi_i(\mathbf{p})\ ,\\ &=\frac{1}{(2\pi)^3}\int_0^\infty dp\,p^2[\,|\psi_{i1}(p)|^2+|\psi_{i2}(p)|^2]\ .\end{aligned} \tag{3.13}$$

Equations (3.11)–(3.13) follow straightforwardly from the two basic identities

$$\int d\hat{\mathbf{r}}\,e^{-i\mathbf{p}\cdot\mathbf{r}}Y^m_{lj}(\hat{\mathbf{r}})=4\pi(-i)^l j_l(pr)Y^m_{lj}(\hat{\mathbf{p}})$$

and

$$\sigma\cdot\hat{\mathbf{r}}Y^m_{l_1j}(\hat{\mathbf{r}})=-Y^m_{l_2j}(\hat{\mathbf{r}})\ .$$

The Dirac optical potential wave function used in (3.7) is discussed in detail in Sec. III A below.

The relationship between the Dirac matrix element represented by (3.7) and the usual DWIA matrix element calculated with Schrödinger wave functions can be seen by recalling a simple derivation of the usual one-body Schrödinger current operator. This operator is often derived through the following steps:

(i) Evaluate the Dirac current operator (3.8) between free positive energy Dirac spinors $\bar{u}(p',s')$ and $u(p,s)$.

(ii) Remove the Pauli spinors contained in the Dirac spinors and multiply the remnants of the Dirac spinors and gamma matrices together to obtain the equivalent operator in Pauli spin space.

(iii) Expand the operator in powers of the momenta divided by the nucleon mass, keeping only the leading orders.

(iv) Fourier transform to obtain an operator in coordinate space.

(v) Evaluate this operator between Schrödinger wave functions.

With the exception of steps (iii) and (iv), this is equivalent to our nonrelativistic calculations which are performed by using Dirac wave functions in (3.7) which have the ratio of upper to lower components fixed at the positive energy plane wave value for each value of the momentum. For the distorted waves, the Fourier amplitudes of the positive energy Dirac spinors are obtained from a microscopic, nonrelativistic calculation,[7,24] whereas for the bound states we project the Dirac wave functions onto the positive-energy space and renormalize to obtain our nonrelativistic limit. It is in this sense that some of the calculations presented below are nonrelativistic.

A. Optical model considerations

The matrix element of (3.7) is addressed in **k** space. The necessary **k**-space distorted waves for the ejected proton are generated from the elastic proton-nucleus half-shell T matrices produced by the computer code WIZARD of Refs. 6, 7, 23, and 24. Both nonrelativistic[23,24] and relativistic[6,7] distorted waves are considered. Construction of the distorted waves and their resolution into separate positive and negative energy parts (in the Dirac approach) follows the methods detailed in Ref. 25. In the following, we explicitly describe these methods for the Dirac approach and for the usual case of outgoing wave boundary conditions for scattering. The modifications necessary for the nonrelativistic approach are indicated, while the case of incoming wave boundary conditions, needed in (3.7), is obtained further on from symmetry considerations. We employ the positive and negative energy Dirac plane-wave basis states of momentum **k** and spin-projection s defined by

$$|\,\mathbf{k}s,\pm\rangle=|\,\mathbf{k},\pm\rangle\,|\,\chi_s\rangle=u^\pm(\mathbf{k})\,|\,\mathbf{k}\rangle\,|\,\chi_s\rangle\ , \tag{3.14}$$

where

$$u^+(\mathbf{k})=N_k\begin{bmatrix}1\\ \dfrac{\sigma\cdot\mathbf{k}}{E_k+m}\end{bmatrix},\quad u^-(\mathbf{k})=N_k\begin{bmatrix}\dfrac{-\sigma\cdot\mathbf{k}}{E_k+m}\\ 1\end{bmatrix}. \tag{3.15}$$

In (3.14), σ is the usual Pauli operator, $|\,\chi_s\rangle$ is a Pauli

spinor of spin-projection s,

$$N_k = \left[\frac{E_k+m}{2E_k}\right]^{1/2}, \tag{3.16}$$

where $E_k=(\mathbf{k}^2+m^2)^{1/2}$. Therefore, $u^{a\dagger}(\mathbf{k})u^b(\mathbf{k})=\delta_{ab}$, where $a,b=\pm$, and $\sum_{a=\pm}u^a(\mathbf{k})u^{a\dagger}(\mathbf{k})=1$. The Dirac kets $|\mathbf{k}\rangle$ satisfy $\langle\mathbf{k}'|\mathbf{k}\rangle=(2\pi)^3\delta^3(\mathbf{k}'-\mathbf{k})$. These basis states follow the conventions of Ref. 25 except for the choice of normalization of $|\mathbf{k}\rangle$. Our choice of $|\mathbf{k}\rangle$ is $(2\pi)^{3/2}$ times the corresponding basis states of Ref. 25 so that we may uniformly follow the convention where phase space for plane wave states is $d^3k/(2\pi)^3$.

WIZARD1 (Refs. 6 and 7) solves the coupled $\mathbf{k}$-space linear integral equations for the Dirac elastic proton-nucleus transition operators $T^{++}(+)$ and $T^{-+}(+)$:

$$\begin{bmatrix}T^{++}((+);\mathbf{k}',\mathbf{k})\\ T^{-+}((+);\mathbf{k}',\mathbf{k})\end{bmatrix}=\begin{bmatrix}U^{++}((+);\mathbf{k}',\mathbf{k})\\ U^{-+}((+);\mathbf{k}',\mathbf{k})\end{bmatrix}+\int\frac{d^3k''}{(2\pi)^3}\begin{bmatrix}U^{++}((+);\mathbf{k}',\mathbf{k}'')U^{+-}((+);\mathbf{k}',\mathbf{k}'')\\ U^{-+}((+);\mathbf{k}',\mathbf{k}'')U^{--}((+);\mathbf{k}',\mathbf{k}'')\end{bmatrix}\times G_D^0((+),k'')\begin{bmatrix}T^{++}((+);\mathbf{k}'',\mathbf{k})\\ T^{-+}((+);\mathbf{k}'',\mathbf{k})\end{bmatrix}, \tag{3.17}$$

which are obtained by taking matrix elements of the Lippmann-Schwinger form of the Dirac equation, written in operator form as

$$T((+))=U((+))+U((+))G_D^0((+))T((+)), \tag{3.18}$$

$$=U((+))+T((+))G_D^0((+))U((+)), \tag{3.19}$$

between the basis states defined above and by resolving the propagator $G_D^0((+))$ with the complete set of basis states, as described in Ref. 7. In (3.17), $T(\mathbf{k}',\mathbf{k})$ and $U(\mathbf{k}',\mathbf{k})$ denote transition operators and optical potentials, respectively, for scattering from an initial Dirac plane-wave basis state of momentum $\mathbf{k}$ to a final basis state of momentum $\mathbf{k}'$. The superscripts $\pm$ determine whether the initial and final basis states are of positive or negative energy, e.g., $T^{-+}((+);\mathbf{k}',\mathbf{k})$ is the scattering operator for the transition from a positive energy state of momentum $\mathbf{k}$ to a negative energy state of momentum $\mathbf{k}'$. Of course, T^{++} is the physical asymptotic transition operator which connects observable states of experimental interest. The operator T^{-+} connects positive energy states to negative energy intermediate states only. WIZARD1 actually solves (3.17) in partial wave form[7] and for the case of outgoing wave boundary conditions, hence the $(+)$ argument of the operators in (3.17)–(3.19). In general we use $+$ or $-$ to denote Dirac positive or negative energy, and $(+)$ or $(-)$ to denote outgoing or incoming (spherical) wave boundary conditions. Thus[7]

$$G_D^0((+);k'')=\begin{bmatrix}(E_k-E_{k''}+i\epsilon)^{-1} & 0\\ 0 & (E_k+E_{k''})^{-1}\end{bmatrix},$$

$$=\begin{bmatrix}g_0^+((+),k'') & 0\\ 0 & g_0^-((+),k'')\end{bmatrix}, \tag{3.20}$$

where we have indicated that the $g_0^{\pm}$ act only in the positive and negative energy spaces. It should be noted that spin indices have been suppressed in (3.17). Each of the elements of the matrices of (3.17) is actually an operator in the two-dimensional Pauli spin space of the ejected particle. In the example of $T^{-+}((+);,\mathbf{k}',\mathbf{k})$ above, the amplitude for a transition from spin projection s to spin projection s' is just $\langle\chi_{s'}|T^{-+}((+);\mathbf{k}',\mathbf{k})|\chi_s\rangle$. It should also be noted that the nonrelativistic transition operator satisfies an equation of the form of (3.18) and that it can be recovered from (3.17) by simply setting $U^{+-}=0$ and then calculating only the top row. This connection of relativistic and nonrelativistic approaches is only so simple in the momentum space approach of Refs. 6, 7, 23, and 24. This is the manner in which we recover the nonrelativistic dynamics.

Given the on-shell and half-shell transition operators $T^{++}(+)$ and $T^{-+}(+)$ for outgoing wave boundary conditions, we can easily construct the corresponding distorted wave $|\psi_{p's'}^{(\pm)},f\rangle$ in $\mathbf{k}$ space. First, we suppress the spin and final nuclear state indices by defining

$$|\psi_{p's'}^{(\pm)},f\rangle=|\psi_{p'}^{(\pm)}\rangle|\chi_{s'}\rangle|\psi_f\rangle, \tag{3.21}$$

where $|\chi_{s'}\rangle$ is a Pauli spinor and $|\psi_f\rangle$ is the final nuclear state vector. If we now take

$$|\psi_{p'}^{(\pm)}\rangle=\Omega_d^{(\pm)}|\mathbf{p}',+\rangle, \tag{3.22}$$

where $\Omega_d^{(\pm)}$ is the Moller operator which produces the distorted wave when it acts on the plane wave, then, since we always start from a positive energy basis state asymptotically, Ω_d can be orthogonally decomposed as

$$\Omega_d=\Omega_d^{++}+\Omega_d^{-+}, \tag{3.23}$$

with

$$\Omega_d^{++}=1+g_0^+((+))T^{++}((+)) \tag{3.24}$$

and

$$\Omega_d^{-+}=g_0^-((+))T^{-+}((+)), \tag{3.25}$$

where we have suppressed the $(\pm)$ superscript.

Employing (3.23)–(3.25) in (3.22), and noting that

$$|\psi_{p'}^{(+)}\rangle=\int\frac{d^3k}{(2\pi)^3}[\,|\mathbf{k},+\rangle\langle\mathbf{k},+|+|\mathbf{k},-\rangle\langle\mathbf{k},-|\,]|\psi_{p'}^{(+)}\rangle, \tag{3.26}$$

one finds that

$$|\psi_{p'}^{(+)}\rangle = \int \frac{d^3k}{(2\pi)^3}[\,|\mathbf{k},+\rangle\psi_{p'}^{(+)}(\mathbf{k},+)+|\mathbf{k},-\rangle\psi_{p'}^{(+)}(\mathbf{k},-)]\,, \tag{3.27}$$

where the Fourier amplitudes on the positive and negative energy spaces are

$$\psi_{p'}^{(+)}(\mathbf{k},+)=\langle\mathbf{k},+\,|\,\psi_{p'}^{(+)}\rangle$$

$$=(2\pi)^3[\delta^3(\mathbf{k}-\mathbf{p}')+g_0^+((+);k)T^{++}((+);\mathbf{k},\mathbf{p}')] \tag{3.28a}$$

$$=(2\pi)^3[\delta^3(\mathbf{k}-\mathbf{p}')-i\pi\delta(E_{p'}-E_k)T^{++}((+);\mathbf{k},\mathbf{p}')+g_0^{PV}(k)T^{++}((+);\mathbf{k},\mathbf{p}')] \tag{3.28b}$$

and

$$\psi_{p'}^{(+)}(\mathbf{k},-)=(2\pi)^3 g_0^-((+),k)T^{-+}((+);\mathbf{k},\mathbf{p}')\,, \tag{3.29}$$

respectively. In (3.28b) we have separated g_0^+ into its delta function and principal parts. Some of the advantages of $\mathbf{k}$ space are evident in (3.27)—(3.29). First, one can easily examine the importance of the negative energy components of the distorted wave for the $(\vec{e},e'p)$ calculation by simply comparing the full $(\vec{e},e'p)$ calculation with one for which T^{-+} is artificially set equal to zero in (3.29). Similarly, one can determine the significance of off-shell information in the distorted wave by simply omitting the g_0^{pv} term of (3.28b). One can also examine the influence on the $(\vec{e},e'p)$ results of different off-shell and nonlocal extrapolations of the optical potential by using the various options available[7,24] in WIZARD1 to produce different half-shell T matrices. Finally, by limiting (3.27) to its first term and using (3.28b) as described earlier, one can compare the nonrelativistic $(\vec{e},e'p)$ predictions with their relativistic counterparts both with and without a negative energy component present in the distorted wave. Similar options are available in the study of the bound state portion of the current matrix element of (3.7).

For convenience and accuracy, we have described the treatment of the distorted wave in terms of the outgoing scattered wave boundary condition case. To completely describe our approach and the manner in which it is actually performed, it is necessary to relate the construction of $\langle p's'(-),\psi_{fP'}\,|$ to the preceding discussion. Now, $|\psi_{p'}^{(-)}\rangle$ is given in operator form by (3.22) where

$$\Omega_d^{(-)}\equiv[1+G_D^0((-))T((-))] \tag{3.30}$$

is the desired Moller wave operator. Given the T matrix, the wave operator can be easily calculated in $\mathbf{k}$ space. This is analogous to the operator form of (3.22)—(3.25). The requisite transition operator $T(-)$ satisfies an optical model equation identical to (3.18) or (3.19) for $T((+))$ except for the change of boundary conditions in the propagator and the presence[26,27] of the adjoint of the optical potential, $U((+))^\dagger$, in place of $U((+))$. These facts may be summarized by the statement[26,27]

$$T(-)=T(+)^\dagger \tag{3.31}$$

which now follows immediately from (3.18) and (3.19). The needed final state is thus obtained from the adjoint of (3.22) and (3.30), which is

$$\langle\psi_{p'}^{(-)}\,|=\langle\mathbf{p}',+\,|\,[1+T((+))G_D^0((+))]\,. \tag{3.32}$$

Equation (3.32) yields $\langle\psi_{p's'}^{(-)},f\,|$ in terms of the solution of (3.18), i.e., the solution of (3.17).

One technical problem remains. The solution of (3.17) yields $T((+);\mathbf{p}',\mathbf{k})$ for fixed $\mathbf{k}$ and all $\mathbf{p}'$, whereas use of (3.32) in evaluating the current matrix element in $\mathbf{k}$ space requires $T((+);\mathbf{p}',\mathbf{k})$ for fixed $\mathbf{p}'$ and all $\mathbf{k}$. In general, $T((+);\mathbf{p},\mathbf{k})$ is not a symmetric function of its arguments. Comparison of one of (3.18) or (3.19) with the transpose (t) of the other, shows that $T((+))^t=T((+))$ if $U((+))^t=U((+))$. In the nonrelativistic case, with no spin-orbit force this is sufficient to make $T((+))$ a symmetric function of its arguments if $U((+))$ is. This is not the case if spin-orbit forces are present. However, the force of (3.18) and (3.19) is preserved in partial wave form so that $T_{LJ}((+);k',k)$ is symmetric if $U_{LJ}((+);k',k)$ is, and this one obtains if the only asymmetry in $U((+))$ is the spin-orbit operator. The symmetric nature of the partial wave $\mathbf{k}$-space optical potential, which implies the same symmetry for $T_{LJ}((+);k',k)$, is a rather general property which is satisfied by all the optical potentials, both relativistic and nonrelativistic, of Refs. 6, 7, 23, and 24. The general feature which underlies these considerations is, of course, the reciprocity relation.[28,29] Although the dynamical equations are not time reversal invariant, due to the non-Hermitian nature of the optical potential, the S matrix and thus the T matrix can be shown to satisfy the reciprocity relation

$$\langle\mathbf{k}'s'\,|\,T\,|\,\mathbf{k}s\rangle=\langle-\mathbf{k},-s\,|\,T\,|\,-\mathbf{k}',-s'\rangle \tag{3.33}$$

which leads to the partial wave symmetry in the momentum arguments discussed above. The general outline of the construction of the requisite distorted waves is now completely described.

B. Calculational procedure

Relevant details of the DWIA calculation of the current matrix element are described in this subsection. We start from the momentum space final state wave function needed in (3.7). Expanding (3.2) in the basis of positive and negative energy plane wave states by the methods of the previous subsection yields

$$\langle\bar{\psi}_{\mathbf{p}'}^{(-)}\,|\,\mathbf{p}\rangle=\sum_{a=\pm}\langle\mathbf{p}',+\,|\,[1+T(+)G_D^0(+)]\,|\,\mathbf{p},a\rangle\bar{u}^{\,a}(\mathbf{p})\,,$$

$$=\sum_{a=\pm}\Omega^{+a}(\mathbf{p}',\mathbf{p})\bar{u}^{\,a}(\mathbf{p})\,, \tag{3.34}$$

where $\bar{u}^a(\mathbf{p})=u^{a\dagger}(\mathbf{p})\gamma^0$ and Ω^{+a} is defined by (3.34). A partial wave expansion of the operator Ω^{+a} is introduced as[7,25]

$$\Omega^{++}(\mathbf{p}',\mathbf{p})=\sum_{LJM}\Omega_{LJ}^{++}(p',p)Y_{L_1J}^M(\hat{\mathbf{p}}')[Y_{L_1J}^M(\hat{\mathbf{p}})]^\dagger ,$$
$$\Omega^{+-}(\mathbf{p}',\mathbf{p})=\sum_{LJM}\Omega_{LJ}^{+-}(p',p)Y_{L_1J}^M(\hat{\mathbf{p}}')[Y_{L_2J}^M(\hat{\mathbf{p}})]^\dagger , \tag{3.35}$$

where $L_1=L$, $L_2=2J-L$, and the partial wave terms are defined in terms of the half-shell T matrix elements for proton-nucleus scattering by expansion of the analogs of (3.28b) and (3.29)

$$\Omega_{LJ}^{+a}(p',p)=(2\pi)^3\left\{\delta_a+\frac{\delta(p-p')}{p^2}S_{LJ}^{++}+4\pi T_{LJ}^{+a}(p',p)PV[g_0^a(p)]\right\} \tag{3.36a}$$

and

$$S_{LJ}^{++}=1-(2\pi)^2E_{p'}ip'T_{LJ}^{++}(p',p') . \tag{3.36b}$$

Here the plane wave final state is obtained by setting S_{LJ} to 1 and T_{LJ} to 0. The factor S_{LJ}^{++} provides on-shell final state distortion and the term involving a principal value provides the off-shell final state distortion. The T matrix elements needed in (3.34)—(3.36) are exactly the ones provided by the WIZARD program. The clean separation of on-shell and off-shell final state effects, as in (3.36), is one of the attractive features of momentum space calculations.

In order to provide a more compact notation, we express the final state wave function in terms of a row vector. Using (3.35) in (3.34) leads to

$$\langle\bar{\psi}_{p's'}^{(-)}|\,\mathbf{p}\rangle=\sum_{LJM}Y_{LJ}^M(\hat{\mathbf{p}}')[\psi_{f1}(p',p)Y_{L_1J}^M(\hat{\mathbf{p}})^\dagger,\psi_{f2}(p',p)Y_{L_2J}^M(\hat{\mathbf{p}})^\dagger] , \tag{3.37a}$$

where

$$\psi_{f1}(p',p)=N_p[\Omega_{LJ}^{++}(p',p)+\lambda_p\Omega_{LJ}^{+-}(p',p)] , \tag{3.37b}$$
$$\psi_{f2}(p',p)=N_p[\lambda_p\Omega_{LJ}^{++}(p',p)-\Omega_{LJ}^{+-}(p',p)] , \tag{3.37c}$$

and $\lambda_p=p/(E_p+m)$.

The current is next expressed in terms of 2×2 matrices of the general form

$$J^\mu(q)=\begin{bmatrix}j_{11}^\mu & j_{12}^\mu\\ j_{21}^\mu & j_{22}^\mu\end{bmatrix} , \tag{3.38}$$

where

$$J^0(q)=(2m)^{-1}\begin{bmatrix}2mF_1 & \boldsymbol{\sigma}\cdot\mathbf{q}F_2\\ \boldsymbol{\sigma}\cdot\mathbf{q}F_2 & -2mF_1\end{bmatrix} \tag{3.39}$$

and

$$\mathbf{J}(q)=(2m)^{-1}\begin{bmatrix}iF_2\boldsymbol{\sigma}\times\mathbf{q} & (2mF_1+\omega F_2)\boldsymbol{\sigma}\\ (-2mF_1+\omega F_2)\boldsymbol{\sigma} & iF_2\boldsymbol{\sigma}\times\mathbf{q}\end{bmatrix} \tag{3.40}$$

and $F_1(q^2)$ and $F_2(q^2)$ are nucleon electromagnetic form factors. In particular, the transverse parts of the vector current, $J_\pm=\hat{\mathbf{e}}_\pm\cdot\mathbf{J}$, take a simple form in terms of spin raising and lowering operators $\sigma_\pm=\hat{\mathbf{e}}_\pm\cdot\boldsymbol{\sigma}$ where $\hat{\mathbf{e}}_\pm=\mp2^{-1/2}(\hat{\mathbf{e}}_x\pm i\hat{\mathbf{e}}_y)$. Note that $i\hat{\mathbf{e}}_\pm\cdot\boldsymbol{\sigma}\times\mathbf{q}=\pm q\sigma_\pm$. We obtain

$$J_\pm(q)=(2m)^{-1}\sigma_\pm\begin{bmatrix}\pm qF_2 & (2mF_1+\omega F_2)\\ (-2mF_1+\omega F_2) & \pm qF_2\end{bmatrix} . \tag{3.41}$$

With these definitions, the desired current matrix element given by (3.7) is expressed as

$$J^\mu=\sum_{LJM}\langle\chi_{s'}|\,Y_{LJ}^M(\hat{\mathbf{p}}')\sum_{r,t=1}^{2}\sum_{\sigma,\sigma'}\int\frac{d^3p}{(2\pi)^3}\psi_{fr}(p',p)[Y_{L_rJ}^M(\hat{\mathbf{p}})]^\dagger|\,\chi_\sigma\rangle\langle\chi_\sigma|\,j_{rt}^\mu(q)\,|\chi_{\sigma'}\rangle$$
$$\times\langle\chi_{\sigma'}|\,\psi_{it}(|\,\mathbf{p}-\mathbf{q}\,|)Y_{l_ij}^m(\Omega_{p-q}) , \tag{3.42}$$

where we have twice utilized the completeness of the Pauli spinors. The spin spherical harmonics can be expressed as follows

$$Y_{LJ}^M(\Omega_p)=\sum_{N,s}\langle LN\tfrac{1}{2}s\,|\,JM\rangle Y_{LN}(\theta_p,\phi_p)\,|\,\chi_s\rangle , \tag{3.43a}$$
$$Y_{LN}(\theta_p,\phi_p)=C(L,N)p_L^N(\cos\theta_p)e^{iN\phi_p} , \tag{3.43b}$$
$$C(L,N)=\left[\frac{2L+1}{4\pi}\frac{(L-N)!}{(L+N)!}\right]^{1/2} . \tag{3.43c}$$

Since $\mathbf{q}$ is parallel to the z axis, the dependence of the integrand of (3.42) upon the azimuthal angle ϕ_p is simply $e^{i(n-N)\phi_p}$, where n and N refer to the z projections of the orbital angular momenta of the bound and scattering (partial wave) states, respectively. Integration over the azimuthal angle therefore produces a factor $2\pi\delta_{nN}$. The remaining integrations have been performed numerically using Gaussian integration. The basic numerical integrals needed are given by

$$I_{rtN}=N_{r+N}\int_0^\infty dp\,p^2\int d(\cos\theta_p)\psi_{fr}(p',p)P^N_{L_r}(\cos\theta_p)\times p^N_{1/t}(\cos\theta_{p-q})\psi_{it}(|\mathbf{p}-\mathbf{q}|)\,, \tag{3.44}$$

where

$$N_{rtN}=(2\pi)^{-2}C(L_r,N)C(l_t,N)\,. \tag{3.45}$$

Once these integrals are determined, the current matrix element becomes simply

$$J^\mu=\langle\chi_{s'}|\sum_{LJM}Y^M_{LJ}(\hat{\mathbf{p}}')\sum_{rt}\sum_{\sigma\sigma'}\sum_N\langle\chi_\sigma|j^\mu_{rt}|\chi_{\sigma'}\rangle\langle L_rN\tfrac{1}{2}\sigma|JM\rangle\langle l_tN\tfrac{1}{2}\sigma'|jm\rangle I_{rtN}\,, \tag{3.46}$$

where (3.38)—(3.41) defines the j^μ_{rt}. This concludes the detailed description of our calculational procedure.

IV. RESULTS

The calculations presented here have been performed for the case of 135 MeV protons ejected from ^{16}O. The final proton energy was chosen to be within the energy range attainable by currently available experimental facilities. In Figs. 3—14, relativistic and nonrelativistic calculations of the five response functions are compared. Figures 3—7 show the response functions for the ejection of a 135 MeV proton from the $1p_{1/2}$ shell of ^{16}O. Figures 8—12 are for the ejection of a 135 MeV proton from the $1p_{3/2}$ shell of ^{16}O. The response functions are plotted as a function of the magnitude of the recoil momentum of the residual nucleus $|\mathbf{p}'-\mathbf{q}|$ at a constant momentum transfer $|\mathbf{q}|=2.64$ fm^{-1}. We have fully examined the behavior of the five response functions as functions of $|\mathbf{p}-\mathbf{q}|$ and $|\mathbf{q}|$ and the figures shown are representative slices of the complete three-dimensional graphs.

The solid line in each figure represents a completely relativistic calculation of the response function using Dirac distorted waves for the ejected proton and Dirac-Hartree[8,9] wave functions for the bound state. Results based on wave functions from Refs. 8 and 9 give essentially the same results. The dot-dashed line represents a nonrelativistic calculation, in the sense described earlier, while the dashed line is the undistorted calculation using the Dirac-Hartree bound state and a Dirac plane wave for the ejected proton. Calculations have also been performed using a nonrelativistic bound state wave function and a relativistic scattering wave function. In all cases, the results of this calculation differ from the fully relativistic calculation by only one or two percent. Thus, the curves shown for the relativistic calculation are also representative of these "semirelativistic" calculations. Figures 3—7 also contain a calculation labeled "on shell" which is represented by a short-dashed line. In this calculation only the pole part of the propagator in the Moller operator is retained; this corresponds to keeping only the on-energy-shell part of the T matrix in the Moller operator. The purpose of this calculation is to provide a rough measure of the sensitivity of the response functions to the off-shell parts of the nucleon-nucleus T matrix in the final state interaction.

Figure 3 shows the longitudinal response function R_L for the $1p_{1/2}$ shell. Here the relativistic calculation is 54% as large as the plane wave result, showing the effect of the loss of flux into other reaction channels. The nonrelativistic R_L is about 20% larger then the relativistic one. We find this to be almost entirely the result of the difference between the nonrelativistic and relativistic dis-

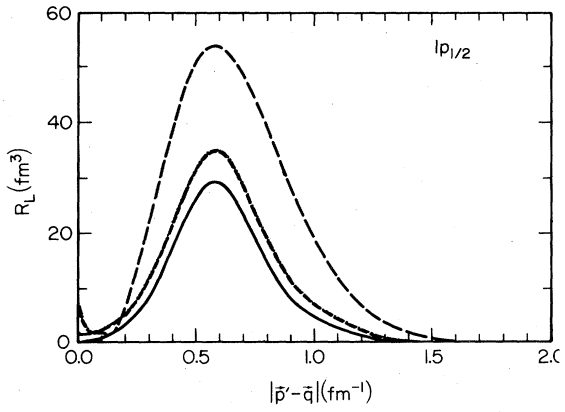

FIG. 3. Longitudinal response function, R_L, as a function of recoil momentum $|\mathbf{p}'-\mathbf{q}|$ for knockout of a 135 MeV proton from the $1p_{1/2}$ shell of ^{16}O. The solid line shows a calculation using a Dirac bound state and a Dirac distorted wave for the ejected proton. The long-dashed line shows the undistorted (plane-wave) result. The dash-dotted line shows a calculation using a Schrödinger bound state and a Schrödinger distorted wave for the ejected proton. The short-dashed line is the "on-shell" calculation described in the text. The meaning of the various lines, as described here, is the same in all subsequent figures.

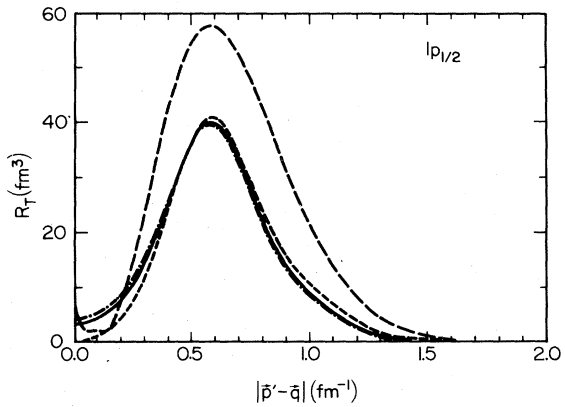

FIG. 4. Transverse response function, R_T, as a function of recoil momentum $|\mathbf{p}'-\mathbf{q}|$ for knockout of a 135 MeV proton from the $1p_{1/2}$ shell of ^{16}O.

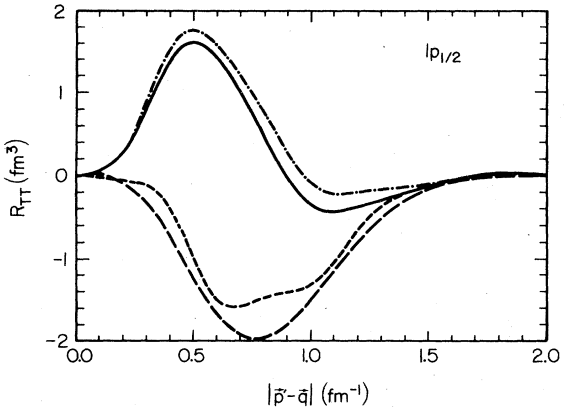

FIG. 5. Transverse-transverse response function, as a function of recoil momentum $|\mathbf{p}'-\mathbf{q}|$ R_{TT}, for knockout of a 135 MeV proton from the $1P_{1/2}$ shell of ^{16}O.

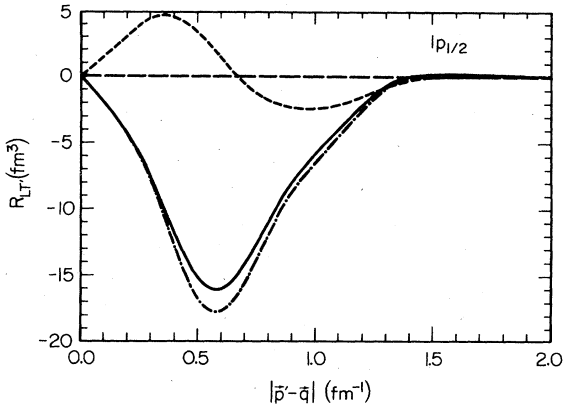

FIG. 7. Helicity dependent longitudinal-transverse response function, $R_{LT'}$, as a function of recoil momentum $|\mathbf{p}'-\mathbf{q}|$ for knockout of a 135 MeV proton from the $1p_{1/2}$ shell of ^{16}O.

torted wave function for the ejected nucleon; the Dirac-Hartree shell-model wave function accounts for only a small part of this difference. The "on-shell" calculation is, coincidentally, almost identical to the nonrelativistic calculation in this case, so that the sensitivity to off-shell effects is also roughly 20%.

Figure 4 shows the transverse response function R_T for the $1p_{1/2}$ shell. As shown in this figure, the relativistic R_T is 68% of the plane wave result. The nonrelativistic R_T is 1% smaller than the relativistic value, indicative of little dependence of this response function on relativistic versus nonrelativistic dynamics. The "on-shell" calculation is very close in size to both of the distorted wave calculations, except for small recoil momenta, so that there appears to be little off-shell sensitivity in this response function. It is interesting to contrast the differences in the various calculations of R_T to those of R_L. While the differences between the relativistic and nonrelativistic calculations of R_T are small, the calculation of R_L which includes relativistic effects is suppressed by a substantial amount relative to the nonrelativistic result. This is the type of change which is necessary to account for the suppression of the longitudinal response function in inclusive (e,e').[12] Note that the effect need not be of the same magnitude in (e,e') as it is in the present $(\vec{e},e'p)$ reaction which includes only one reaction channel. The interesting feature of this suppression is that it is due to dynamical relativistic effects in the final state interaction. This can be seen by noting that the relativistic and "semirelativistic" calculations, which differ only by whether the bound state wave function is relativistic or nonrelativistic, are essentially the same. Thus, relativistic bound state effects are small in both cases.

Figure 5 shows the transverse-transverse interference response function R_{TT} for the $1p_{1/2}$ shell. Notice that this response function is small compared to R_L and R_T, being only about 6% at large as R_L. The magnitude of the relativistic calculation is about 20% less than the plane wave result but is of opposite sign. The relativistic and nonrelativistic R_{TT} values differ by about 10%. The "on-shell" calculation differs both in sign and shape from the other two distorted wave calculations so that this response function seems to be especially sensitive to off-shell effects. Unfortunately, this response function is suf-

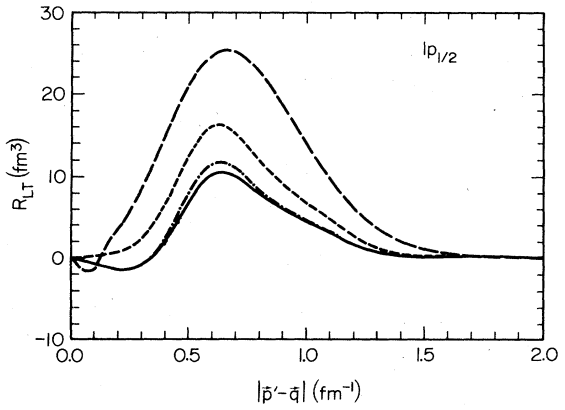

FIG. 6. Longitudinal-transverse response function, R_{LT}, as a function of recoil momentum $|\mathbf{p}'-\mathbf{q}|$ for knockout of a 135 MeV proton from the $1p_{1/2}$ shell of ^{16}O.

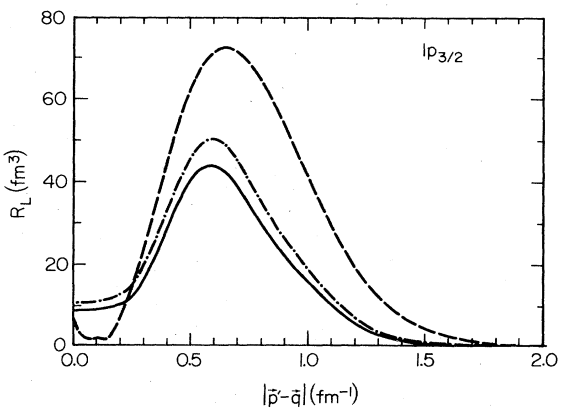

FIG. 8. Longitudinal response function, R_L, as a function of recoil momentum $|\mathbf{p}'-\mathbf{q}|$ for knockout of a 135 MeV proton from the $1p_{3/2}$ shell of ^{16}O.

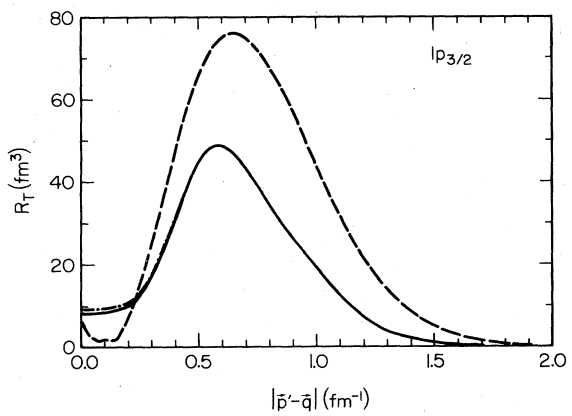

FIG. 9. Transverse response function, R_T, as a function of recoil momentum $|\mathbf{p}'-\mathbf{q}|$ for knockout of a 135 MeV proton from the $1p_{3/2}$ shell of ^{16}O.

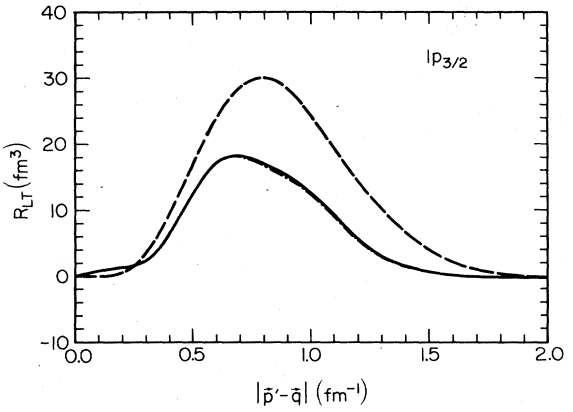

FIG. 11. Longitudinal-transverse response function, R_{LT}, as a function of recoil momentum $|\mathbf{p}'-\mathbf{q}|$ for knockout of a 135 MeV proton from the $1p_{3/2}$ shell of ^{16}O.

ficiently small relative to the other response functions that it will be difficult to extract experimentally. Furthermore, the experimental determination of R_{TT} requires that the ejected proton be detected out of the electron scattering plane, as discussed in Sec. II.

Figure 6 shows the longitudinal-transverse interference response function R_{LT} for the $1p_{1/2}$ shell. The relativistic calculation is only about 40% as large as the plane wave, showing a greater sensitivity to final state interaction effects than either R_L or R_T. On the other hand, the relativistic and nonrelativistic calculations differ by about 10%, showing relativistic dynamic sensitivity intermediate between R_L and R_T. The "on-shell" calculation is about 55% larger than the relativistic result suggesting that this response function is quite sensitive to the off-shell character of the final state interaction. R_{LT} is about half as large as R_L and so should be experimentally observable with good accuracy (see Sec. II).

Figure 7 shows the helicity dependent longitudinal-transverse interference response function $R_{LT'}$ for the $1p_{1/2}$ shell. This response function can only be measured using a polarized electron beam. The plane wave value of $R_{LT'}$ is identically zero for all recoil momenta since this response function can only be nonzero if the ejected proton experiences final state interactions with the residual nucleus. Therefore, $R_{LT'}$ exists only as a result of the final state interaction. Consistent with this statement, the relativistic and nonrelativistic distorted wave results are nonzero and differ by about 10%, indicating dependence on relativistic effects similar to that of R_{LT}. The "on-shell" calculation differs considerably from the two distorted wave calculations. This suggests that the interference structure functions may be, in general, quite sensitive to off-shell effects. Since $R_{LT'}$ is 55% of R_L it is quite possible that an intense polarized electron beam will allow $R_{LT'}$ to be extracted from the cross section data. However, this can be accomplished only with an out-of-plane spectrometer, as discussed in Sec. II.

Figures 8—12 show that the results for the $1p_{3/2}$ shell are similar to those of the $1p_{1/2}$ shell. There is, however, an interesting difference between the calculations in the two shells. Distorted wave calculations, both relativistic

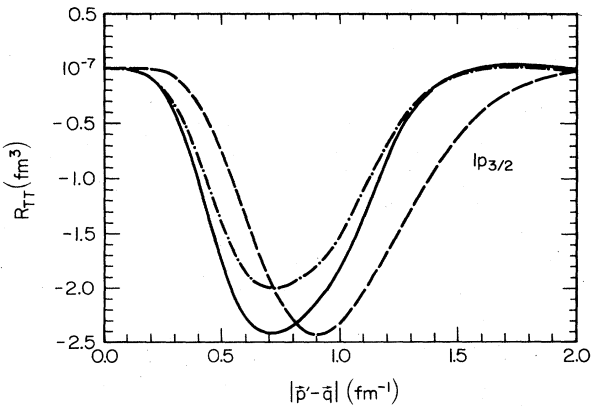

FIG. 10. Transverse-transverse response function, as a function of recoil momentum $|\mathbf{p}'-\mathbf{q}|$ R_{TT}, for knockout of a 135 MeV proton from the $1p_{3/2}$ shell of ^{16}O.

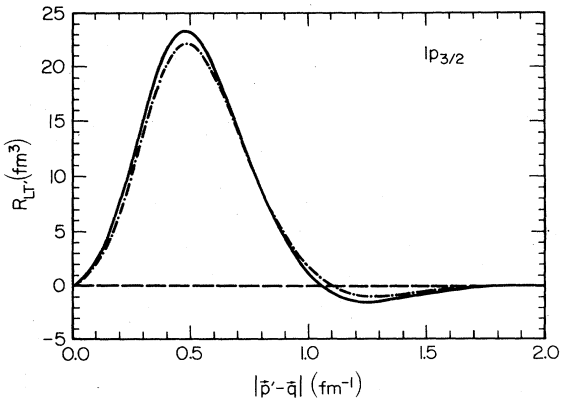

FIG. 12. Helicity dependent longitudinal-transverse response function, $R_{LT'}$, as a function of recoil momentum $|\mathbf{p}'-\mathbf{q}|$ for knockout of a 135 MeV proton from the $1p_{3/2}$ shell of ^{16}O.

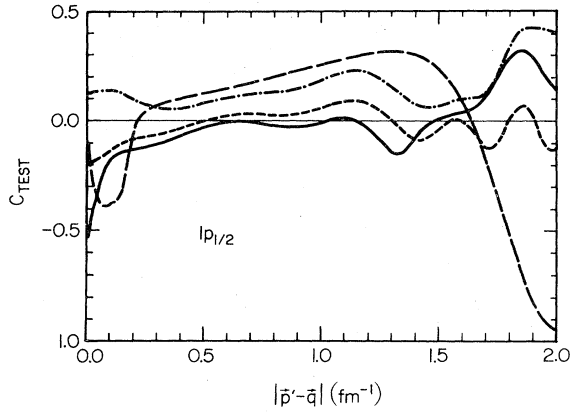

FIG. 13. C_{test} as a function of the recoil momentum for the $1p_{1/2}$ shell of ^{16}O. See the text.

and nonrelativistic, of R_{TT} and $R_{LT'}$ in the $1p_{1/2}$ shell produce opposite signs relative to their analogous calculations in the $1p_{3/2}$ shell. However, the sign of R_{LT} is the same in both shells. The existing cross section[30] data indicate that R_{LT} changes sign when going from one shell to the other. Nonrelativistic calculations[2] have been able to reproduce this feature by adjusting the imaginary part of the spin-orbit contribution to the optical potential. This freedom is not available within the context of our microscopic treatment of the proton distorted waves. However, recent work has suggested that a more complex approach based on meson theory is needed at low proton energy to produce a good description of proton-nucleus elastic scattering.[31–33] It is possible that these improvements to the optical potential at low energy would remove this deficiency in the present calculations. An implementation of the improved proton distortion for momentum-space calculations is being developed and this is expected to lead to an improved analysis in the near future.

Another, possibly related, problem is current conservation. In deriving the expression for the $(\vec{e},e'p)$ cross section, it is assumed that the electromagnetic current is conserved, which implies that

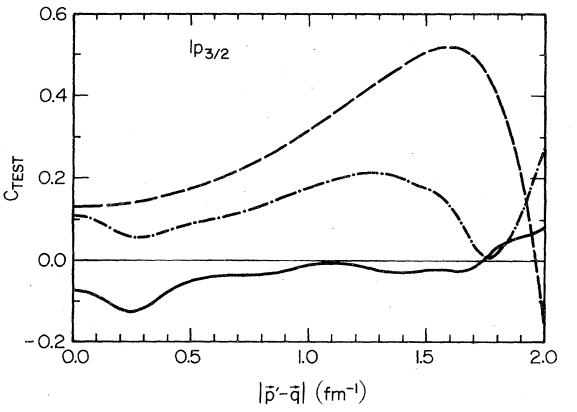

FIG. 14. C_{test} as a function of the recoil momentum for the $1p_{3/2}$ shell of ^{16}O. See the text.

$$J^0=\mathbf{q}\cdot\mathbf{J}/\omega=|\mathbf{q}|J_L/\omega\ , \tag{4.1}$$

where J_L is the longitudinal component of the three-vector current. We employed this constraint in Sec. II to write R_L entirely in terms of J^0. However, one must obtain the same longitudinal response function R_L by employing instead the longitudinal current J_L and using (4.1) to eliminate J^0, if current is conserved. Thus, as a rough test of the effect of current nonconservation, we may compare the calculations of the longitudinal response function based on the two different alternatives (J^0 or J_L). For clarity, the response function calculated on the basis of J_L is referred to as $\tilde{R}_L$. Figures 13 and 14 show the quantity

$$C_{\text{test}}=\frac{R_L-\tilde{R}_L}{R_L+\tilde{R}_L} \tag{4.2}$$

for both the $1p_{1/2}$ and $1p_{3/2}$ shells. The line types in these figures correspond to those used in the figures displaying the response functions. Clearly, the constraint of current conservation requires C_{test} to be zero for all recoil momenta. The present calculations indicate violations of current conservation by as much as 40%, by this measure. This is not unexpected due to the orthogonality problems which show up in DWIA calculations of all types. Moreover, all DWIA calculations omit two-body currents and meson exchange currents. However, it may be worth noting that the effects of the violation of current conservation for the relativistic calculations in the region of the peaks in the response functions is 10% or less (by this measure) so that the calculations may be more reliable than expected *a priori*. In principle, it is possible to restore current conservation in a dynamically meaningful way, but that requires an extension of the current approach which is beyond the scope of this paper. While it is important to determine whether or not such an extension will introduce any new features in the response functions, there is no reason to expect it to result in any qualitative changes to the results presented here.

V. CONCLUSIONS

In this paper, we have presented the results of a detailed study of the influence of the hadronic dynamics on the five response functions which characterize the $(\vec{e},e'p)$ reaction. Within the framework of a distorted wave impulse approximation, we cleanly separated and gauged (1) the effects of relativistic versus nonrelativistic dynamics in both the treatment of the bound state and the treatment of final state interactions, (2) the importance of the final state interaction, and (3) the importance of off-shell versus the (better constrained) on-shell part of the final state interaction. We have also proposed a measure of the ambiguity introduced in DWIA calculations by the violation of current conservation and we have used it to obtain at least some indication of the impact of current nonconservation upon our calculations.

Before summarizing the detailed information obtained from our studies of the five response functions, four of our results deserve special note:

(1) In all five response functions we find that the effects

of relativistic (as opposed to nonrelativistic) dynamics on the calculated results arise almost entirely from the final state interaction of the ejected proton. Relativistic effects arising from the bound state dynamics are small.

(2) The method we have used to estimate the uncertainty introduced into the calculations by the violation of current conservation appears to indicate that such effects may be at the 10% level when the response functions are near their maxima.

(3) We have found a 20% suppression of the longitudinal response function R_L with the use of relativistic as opposed to nonrelativistic dynamics in the description of the final state interaction. Since no such effect is seen for the transverse response function R_T, this is also a 20% reduction of R_L relative to R_T. It may be speculated that this result is indicative of the source of at least part of the observed suppression of the longitudinal response function in quasielastic (e,e').

(4) For the five response functions, we find large effects due to the final state interaction. This indicates that a careful, controlled treatment of the final state interaction is required prior to the extraction of spectroscopic information from the (e,e'p) response functions.

Our analysis indicates that measurement of the complete set of five response functions would prove valuable in a theoretical separation of the relativistic versus nonrelativistic dynamical effects from the on- and off-shell effects of the final state interaction, and in the separation of these from the nuclear structure dependent information. Our results indicate the following picture. The response function R_T is virtually independent of the choice of relativistic versus nonrelativistic dynamics, as well as the off-shell part of the final state interaction. Analysis of this response function apparently requires as input only accurate information concerning the on-shell final state interaction. All of the interference response functions (R_{TT}, R_{LT}, and $R_{LT'}$) are extremely sensitive to the off-shell part of the final state interaction, but show a sensitivity to relativistic effects only at the 10% level. Moreover, the character of the off-shell sensitivity is very different for each of the three interference response functions. Thus, these response functions can be used as a "proving ground" for the treatment of the off-shell part of the final state interaction. Finally, the longitudinal response function appears to be about equally sensitive to off-shell and relativistic effects. Given control of the former via the interference response functions, R_L provides for elucidation of the latter. The point here, of course, is that the different dynamical dependences of the five response functions provide an opportunity for untangling both the important dynamical mechanisms and the structure information.

Despite the above results, several caveats are in order. A measure of caution is needed in drawing firm conclusions from our calculations, or for that matter, from any DWIA calculation of the $(\vec{e},e'p)$ reaction, due to the severe approximations made in regard to the appropriate current operator. This concern manifests itself most directly as a violation of current conservation in such treatments. Although our estimates suggest that the error from this source may not be too large, further investigation is certainly necessary. This, along with the failure of the calculations presented here to reproduce the change in sign of R_{LT} between the $1p_{1/2}$ and $1p_{3/2}$ shells, augers for a deeper, more fundamental approach. Furthermore, it is well known that meson exchange currents make important contributions in the $(\vec{p},\gamma)$ reaction, to which we intend to extend our considerations. For these reasons, a consistent treatment, rooted in meson theory, of the bound state, the current operator, and the final distorted wave[32,33] is currently under investigation. Only within the context of such a fundamental theoretical grounding can the current matrix elements be properly addressed. Finally, two relatively minor points should also be kept in mind when comparing our calculations to experimental data. In our investigations, we have, for simplicity, neglected Coulomb distortion of the ejected proton and we have taken the nucleus to be infinitely heavy. Neither of these truncations is an integral part of our approach and we intend to remove them in our future investigations.

ACKNOWLEDGMENTS

The authors would like to acknowledge H. Fearing for a valuable conversation. Support of the United States Department of Energy is gratefully acknowledged.

*Present address: TRIUMF, 4004 Wesbrook Mall, Vancouver, British Columbia, Canada V6T 2A3.

[1]S. Boffi, C. Giusti, F. D. Pacati, and S. Frullani, Nucl. Phys. **A319**, 416 (1979).
[2]S. Boffi, C. Giusti, and F. D. Pacati, Nucl. Phys. **A336**, 437 (1980); Nucl. Phys. **A386**, 599 (1982).
[3]C. Giusti and F. D. Pacati, Nucl. Phys. **A336**, 427 (1980).
[4]J. A. McNeil, J. R. Shephard, and S. J. Wallace, Phys. Rev. Lett. **50**, 1439 (1983); J. R. Shephard, J. A. McNeil, and S. J. Wallace, *ibid.* **50**, 1443 (1983).
[5]B. C. Clark, S. Hama, R. L. Mercer, L. Ray, and B. D. Serot, Phys. Rev. Lett. **50**, 1644 (1983).
[6]M. V. Hynes, A. Picklesimer, P. C. Tandy, and R. M. Thaler, Phys. Rev. Lett. **52**, 978 (1984).
[7]M. V. Hynes, A. Picklesimer, P. C. Tandy, and R. M. Thaler, Phys. Rev. C **31**, 1438 (1985).
[8]C. J. Horowitz and B. D. Serot, Nucl. Phys. **A368**, 503 (1981).
[9]L. D. Miller, Phys. Rev. C **14**, 706 (1976).
[10]L. D. Miller and A. E. S. Green, Phys. Rev. C **5**, 241 (1972).
[11]L. D. Miller, Phys. Rev. Lett. **51**, 1733 (1983).
[12]Z. E. Meziani *et al.*, Phys. Rev. Lett. **52**, 2130 (1984).
[13]B. Frois, Nucl. Phys. **A434**, 57 (1985).
[14]R. Rosenfelder, Ann. Phys. (N.Y.) **128**, 188 (1980).
[15]J. V. Noble, Phys. Rev. Lett. **46**, 412 (1981).
[16]G. Do Dang and N. Van Giai, Phys. Rev. C **30**, 731 (1984).
[17]T. W. Donnelly, *Nuclear and Subnuclear Degrees of Freedom and Lepton Scattering* (Erice Lectures, Erice, Italy, 1984).
[18]T. W. Donnelly and J. D. Walecka, Annu. Rev. Nucl. Sci. **25**,

329 (1975).
[19]T. W. Donnelly, in *Proceedings of Workshop on Perspectives in Nuclear Physics at Intermediate Energies,* edited by S. Boffi, C. Ciofi degli Atti, and M. M. Giannini (World-Scientific, Trieste, 1984).
[20]J. D. Bjorken and S. D. Drell, *Relativistic Quantum Mechanics* (McGraw-Hill, New York, 1964).
[21]F. E. Close, *An Introduction to Quarks and Partons* (Academic, London, 1979), p. 294.
[22]A. Picklesimer and R. M. Thaler, Phys. Rev. C **23**, 42 (1981); A. Picklesimer, *ibid.* **24**, 1400 (1981).
[23]A. Picklesimer, P. C. Tandy, R. M. Thaler, and D. H. Wolfe, Phys. Rev. C **29**, 1582 (1984).
[24]A. Picklesimer, P. C. Tandy, R. M. Thaler, and D. H. Wolfe, Phys. Rev. C **30**, 1861 (1984).
[25]M. V. Hynes, A. Picklesimer, P. C. Tandy, and R. M. Thaler Phys. Rev. C (to be published).
[26]See, e.g., Ref. 27. Also, note that in the case that the optical potential is Hermitian analytic, $U((+))^{\dagger}=U((-))$, the form of the integral equation for $T((-))$ becomes that of (3.18) and (3.19) with only the boundary conditions changed. This is the justification for the notation $T((-))$.
[27]A. Picklesimer, P. C. Tandy, and R. M. Thaler, Phys. Rev. C **25**, 1215 (1982).
[28]See, e.g., Ref. 29 for a discussion of time reversal and the reciprocity theorem. Although the case of non-Hermitian potentials is not discussed there, the generalization is straightforward from the modified form of the S matrix.
[29]W. M. Gibson and B. R. Pollard, *Symmetry Principles in Elementary Particle Physics* (Cambridge University, Cambridge, 1976).
[30]M. Bernheim *et al.*, Nucl. Phys. **A375**, 381 (1982).
[31]S. J. Wallace, Proceedings of the LAMPF Workshop on Dirac Approaches to Nuclear Physics, 1985 (unpublished).
[32]J. A. Tjon and S. J. Wallace, Phys. Rev. Lett. **54**, 1357 (1985).
[33]J. A. Tjon and S. J. Wallace, submitted to Phys. Rev. C.